Insight into the Active-Site Structure and Function of Cytochrome Oxidase by Analysis of Site-Directed Mutants of Bacterial Cytochrome *aa₃* and Cytochrome *bo*

Jonathan P. Hosler,[1] Shelagh Ferguson-Miller,[1] Melissa W. Calhoun,[2] Jeffrey W. Thomas,[2] John Hill,[2] Laura Lemieux,[2] Jixiang Ma,[2] Christos Georgiou,[2] John Fetter,[1] James Shapleigh,[2,3] Mary M. J. Tecklenburg,[1,4] Gerald T. Babcock,[1] and Robert B. Gennis[2]

Cytochrome *aa₃* of *Rhodobacter sphaeroides* and cytochrome *bo* of *E. coli* are useful models of the more complex cytochrome *c* oxidase of eukaryotes, as demonstrated by the genetic, spectroscopic, and functional studies reviewed here. A summary of site-directed mutants of conserved residues in these two enzymes is presented and discussed in terms of a current model of the structure of the metal centers and evidence for regions of the protein likely to be involved in proton transfer. The model of ligation of the heme *a₃* (or *o*)-Cu_B center, in which both hemes are bound to helix X of subunit I, has important implications for the pathways and control of electron transfer.

INTRODUCTION

Mitochondrial cytochrome *c* oxidase has been studied intensively by a variety of spectral and biochemical techniques, but has not been amenable to analysis by molecular genetic methods because of the complexity of its structure and gene organization. It is thus a welcome discovery that a number of genetically accessible and structurally simpler bacterial oxidases show strong homology to the mitochondrial enzyme and provide useful model systems for examining its catalytic mechanism. The application of site-directed mutagenesis, along with highly developed spectral

methodologies, has led to new insight into the structural features of the active site of cytochrome oxidase (Hosler *et al.*, 1992b; Lemieux *et al.*, 1992; Minagawa *et al.*, 1992; Shapleigh *et al.*, 1992b).

The *aa₃*-type cytochrome *c* oxidases are members of a large superfamily of proton-pumping respiratory oxidases (Saraste, 1990; Gennis, 1991). This group of enzymes has in common a heme-copper binuclear center, the catalytic site where oxygen is reduced to water. The oxidase superfamily was first revealed by the extraordinary similarity of the deduced amino acid sequences of subunit I of bovine cytochrome *c* oxidase and subunit I of the *bo*-type ubiquinol oxidase of *E. coli* (Chepuri *et al.*, 1990b). Approximately 40% of the residues of the bovine subunit are identical to those in the subunit from the *E. coli* oxidase. Considerable biophysical characterization over the last few years has firmly established the close relationship of these enzymes (Salerno *et al.*, 1989; Chepuri *et al.*, 1990a; Salerno *et al.*, 1990; Puustinen *et al.*, 1991; Hill *et al.*, 1992; Minghetti *et al.*, 1992). It is now evident that

[1] Departments of Biochemistry and Chemistry, Michigan State University, East Lansing, Michigan 48824.
[2] School of Chemical Sciences, University of Illinois, Urbana, Illinois 61801.
[3] Current address: Section of Microbiology, Cornell University, Wing Hall, Ithaca, New York, 14853.
[4] Current address: Department of Chemistry, Central Michigan University, Mt. Pleasant, Michigan 48859.

Table I. Characteristics of *Rhodobacter sphaeroides* cytochrome aa_3

Subunit	Structure		
	Mol. wt (kDa)		Amino acid sequence homology to bovine cytochrome aa_3
I	62.1		52% identical, 76% similar
II	32.9		39% identical, 63% similar
III	30.1		49% identical, 71% similar
Activity	$TN_{max} = 1{,}800\,s^{-1}$; biphasic dependence on mammalian cytochrome c		
UV-VIS spectrum	Soret $max_{red} = 444.5\,nm$ (bovine $= 443\,nm$); α band $max_{red} = 606\,nm$ (bovine $= 604\,nm$) Extinction coefficients same as bovine		
Proton pumping	$0.7 \pm 0.2 H^+/e^-$ (same as bovine)		

there is a wide range of diversity within the oxidase superfamily encompassing the heme type that is present (heme A, B, or O) as well as the substrate utilized (cytochrome c or quinol). Despite this diversity, the eukaryotic oxidases and the large variety of related prokaryotic oxidases appear to share underlying structural features as well as common catalytic mechanisms. Most bacterial oxidases that have been examined so far are members of this superfamily. The most notable exception is the *bd*-type ubiquinol oxidase, which shares no sequence homology with the heme-copper oxidases and, indeed, contains no copper (Anraku and Gennis, 1987; Kahlow *et al.*, 1991).

This article will summarize our current knowledge of two bacterial oxidases, cytochrome aa_3 of *Rhodobacter sphaeroides* and cytochrome *bo* of *Escherichia coli*. Studies of these two enzymes provide complementary information regarding the organization of the metal centers in subunit I.

Cytochrome aa_3 (Cytochrome c Oxidase) of *Rhodobacter sphaeroides*

1.1. Physical and Spectral Properties of the Native Enzyme

In order to apply mutational analysis to this enzyme it was necessary to clone, sequence, and delete the genes from the chromosome, to reintroduce the genes on a plasmid, as well as to purify and characterize the enzyme. The results of these studies revealed that this bacterial enzyme is highly homologous to

mammalian mitochondrial cytochrome c oxidase, including the ability to pump proton in the purified reconstituted state (Table I). The three subunits of this bacterial enzyme are about 70% similar to the mitochondrially encoded subunits of beef heart oxidase (Cao *et al.*, 1991, 1992; Shapleigh and Gennis, 1992). Kinetic and spectral characteristics also show strong resemblance (Hosler *et al.*, 1992b; Shapleigh *et al.*, 1992a,b). Resonance Raman spectra of the bacterial enzyme correspond closely to those of beef heart oxidase (Hosler *et al.*, 1992b; Shapleigh *et al.*, 1992b), allowing unequivocal interpretation of several resonance Raman modes that reflect interactions of the hemes with the protein. An interesting difference between the beef and *Rb. sphaeroides* enzymes is revealed by EPR spectroscopy: a shift in the g_z value for heme *a* from 3.03 in beef to 2.83 in *Rb. sphaeroides* (Hosler *et al.*, 1992b). A similar shift is observed in the g_z value of heme *a* of cytochrome aa_3 from *Paracoccus denitrificans* (Erecinska *et al.*, 1979; Albracht *et al.*, 1980). From comparisons with model compounds and with other heme proteins, it can be concluded that this shift results from an increased strength of the hydrogen bonding to one or both histidine ligands of heme *a*. Such an effect could also account for the slight red shift of the heme *a* spectrum of *Paracoccus* and *Rb. sphaeroides* relative to that of the bovine oxidase (Hosler *et al.*, 1992b).

Another anomaly in the EPR spectrum is due to the presence of manganese at substoichiometric amounts in the purified enzyme. This is also observed with the oxidase isolated from *P. denitrificans* (Seelig
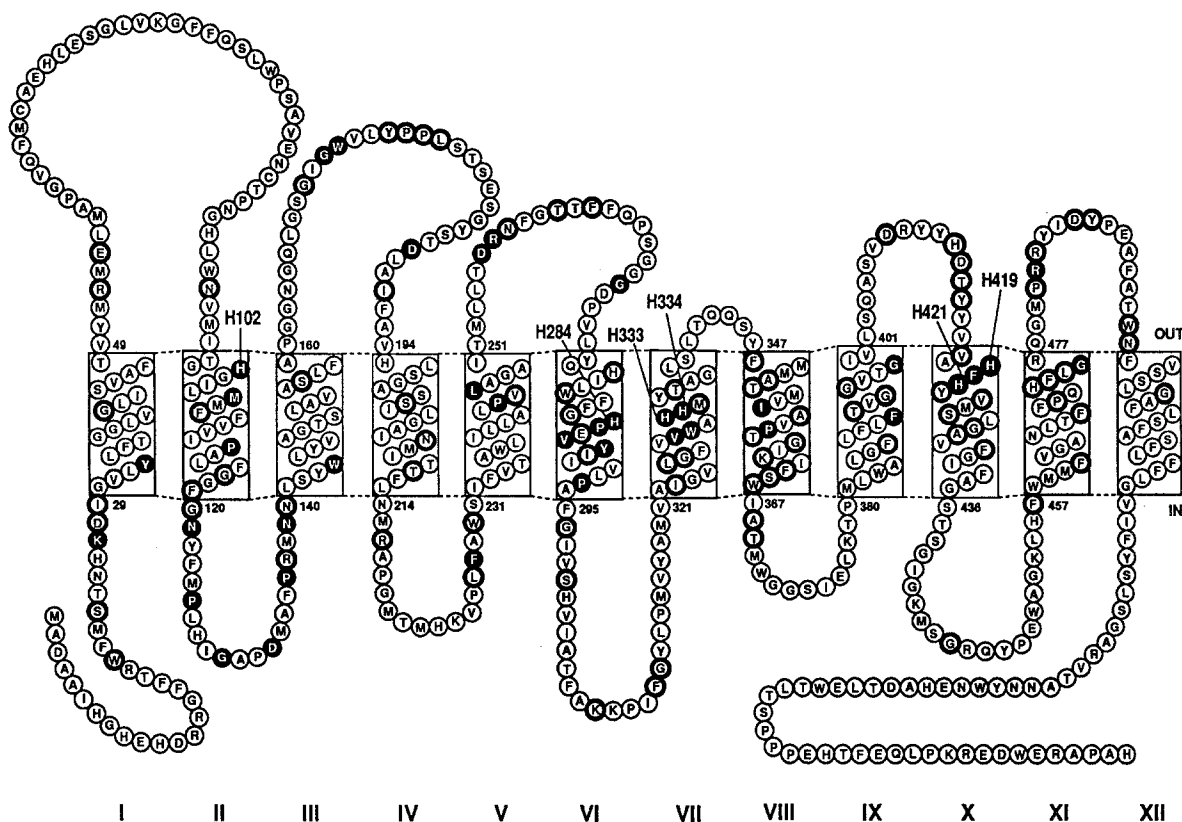
Fig. 1. The amino acid sequence of subunit I of the *Rb. sphaeroides* oxidase showing 12 predicted transmembrane helices. The six conserved histidines labelled in the transmembrane helices serve as metal ligands. Other completely conserved residues are shown as filled circles; highly conserved residues are in bold open circles.

et al., 1981; Haltia, 1992). Treating the *Rb. sphaeroides* oxidase with high concentrations of chelating agents does not remove the manganese. However, three site-directed mutants of the enzyme are found to no longer bind manganese: *His*411*Asn*, *His*411*Ala*, and *Asp* 412*Asn*. Therefore, manganese binding appears to involve residues in the highly conserved hydrophilic loop between helices IX and X (Fig. 1), which is likely to be close to the location of both hemes *a* and *a₃* (Hosler *et al.*, 1992a). Proximity of this site to Cu_A, located within subunit II, is suggested by studies of Haltia (1992), who showed changes in the EPR signal of manganese upon reduction of Cu_A. The low occupancy ($\sim 5\%$) of this binding site by Mn may be an indication that another metal is present, such as magnesium or zinc.

Fourier transform infrared (FTIR) analysis of the *Rb. sphaeroides* enzyme in the bacterial membrane provides another powerful spectroscopic tool for examining the metal centers. Caughey (Caughey *et al.* 1970; Einarsdóttir *et al.*, 1988) and Alben (Alben

et al., 1981; Fiamingo *et al.*, 1982, 1986, 1990), and colleagues have identified stretching frequencies associated with CO binding to heme *a₃* and Cu_B in beef heart oxidase, and essentially identical frequencies are found for the *Rhodobacter* enzyme (Shapleigh *et al.*, 1992a). An FTIR difference spectrum of CO bound to the oxidase from *Rb. sphaeroides* is shown in Fig. 2. Disruption of the binuclear (heme a_3–Cu_B) center causes broadening and major shifts in the CO stretching frequencies. Subtle shifts are also observed with some mutant forms. These signals can be measured *in situ* using isolated membranes, without purifying the oxidase, and give important complementary information to that obtained by EPR and resonance Raman spectroscopy.

Although the purified bacterial oxidase is extremely active ($V_{max} = 1800\,sec^{-1}$ with soluble cytochrome *c*), measurements of its activity in the cytoplasmic membrane are complicated by the presence of another cytochrome *c* oxidase in *Rb. sphaeroides*, a *cb*-type oxidase. Efforts to prepare a
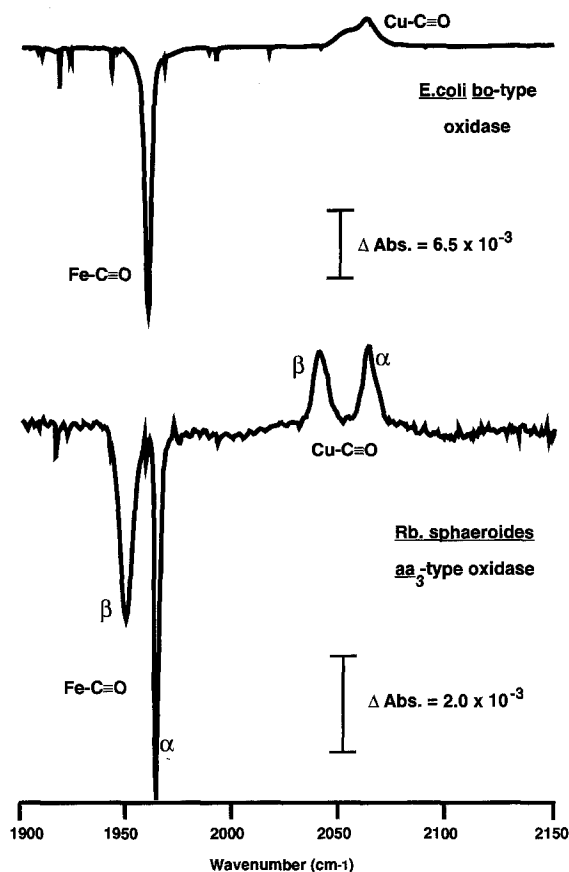
Fig. 2. Low-temperature Fourier transform infrared (FTIR) difference spectra of CO bound to the *Rb. shaeroides* or *E. coli* oxidases in their respective membranes. Each spectrum was obtained by subtracting a spectrum obtained during continuous photolysis, where CO is bound to Cu_B, from the spectrum obtained in the dark, where CO is bound to the heme iron. Hence, the negative peak is due to the CO stretching of Fe–CO. There are two distinct conformational states of the *Rb. sphaeroides* binuclear center (α and β) reported by this technique, just as found with the bovine oxidase. (Fiamingo *et al.*, 1986). This is not observed with the *E. coli* oxidase. Contributions of the *cb*-type oxidase to the aa_3-type oxidase spectrum are discussed in Shapleigh *et al.* 1992a.

bacterial strain deleted in this enzyme are currently under way. In spite of this complication, it is clear that cytochrome aa_3 of *Rb. sphaeroides* in the native membrane is strongly associated with a membrane-bound cytochrome *c* that permits high activity with TMPD alone (Hosler *et al.*, 1992b). This cytochrome *c* is removed during purification and likely resembles cytochrome c_{552} of *P. denitrificans* (Berry and Trumpower, 1985; Steinrücke *et al.*, 1991a). The physiological role of the bound cytochrome *c* is not clear, since kinetic analyses show that the membrane-bound oxidase has the additional ability to react with

soluble cytochrome *c* with relatively high affinity, in contrast to the caa_3 enzymes of *Thermus thermophilus* (Yoshida and Fee, 1984) and PS3 (Nicholls and Sone, 1984).

1.2 The COXII/COXIII Operon Contains ORFs Resembling cox10 and cox11 of Yeast

The *cox*I (*cta*D) gene encoding subunit I of the *Rb. sphaeroides* oxidase is not adjacent to the genes encoding subunits II or III (Shapleigh and Gennis, 1992). The latter are together on a separate COXII/COXIII operon in which two open reading frames, coding for proteins homologous to COX10 and COX11 in yeast (Nobrega *et al.*, 1990; Tzagoloff *et al.*, 1990), are present between *cox*II (*cta*C) and *cox*III (*cta*E) (Cao *et al.*, 1992). These proteins apparently function to assemble the aa_3-type cytochrome *c* oxidase in both yeast and *Rb. sphaeroides*, perhaps assisting protein folding or through a role in heme A biosynthesis or metal insertion. Homologous proteins are found in *P. denitrificans* (Steinrücke *et al.*, 1991b), which has an operon structure similar to that of *Rb. sphaeroides* (Raitio *et al.*, 1987). Homologues of COX10 have also been identified in *E. coli* (see Section 2.1) and in *B. subtilis* (Saraste *et al.*, 1991).

1.3. The Metal Center Ligands in COXI

The basis for our initial efforts in mutational analysis was evidence that heme *a*, heme a_3, and Cu_B are ligated by residues in COXI and that the ligands involved are predominantly histidines (see Wikstrom *et al.* 1985; Saraste, 1990); analysis of the amino acid sequences of over 30 different cytochrome oxidases reveals six totally conserved histidines in COXI (Fig. 1), these histidines are the obvious candidates to fulfil the metal liganding function.

Measurement of the activity of the purified mutant forms of the *Rb. sphaeroides* oxidase supports the idea that the totally conserved histidines of COXI play a critical role, since alteration of any one of them creates an inactive enzyme. Resonance Raman and visible spectra provide strong evidence for the assignment of *His*102 and *His*421 as the heme *a* ligands, *His*333 and *His*334 as Cu_B ligands, and *His*284 or *His*419 as the ligand of heme a_3 (Table II) (Shapleigh *et al.*, 1992b). Further evidence regarding the heme a_3 ligand has been obtained from resonance Raman studies of mutant forms of the enzyme at different

Table II. Mutational Analysis of Subunit I of Cytochrome *c* Oxidase from *Rhodobacter sphaeorides*

Subunit I residue[d]	Helix	Mutation(s)	Phenotype of mutant oxidase[a]	Proposed role of residue
*His102	II	N	Unstable protein; loss of α-band absorbance	Heme *a* ligand
His277	VI	L[b]	Severe disruption of a_3-Cu$_B$	Unknown
*His284	VI	A	Severe disruption of a_3-Cu$_B$, but iron-his stretch of a_3 detectable; altered CO binding	Possible Cu$_B$ ligand
Glu286	VI	Q, D[b]	Low CO binding to heme a_3, but normal FTIR	Possible resting state bridging ligand
*Tyr288	VI	F	Severe disruption of a_3-Cu$_B$, but iron-his stretch of a_3 detectable; altered CO binding	Possible Cu$_B$ ligand
*His333	VII	N	Largely intact a_3-Cu$_B$ center by RR, EPR, but low CO binding and altered Cu$_B$ by FTIR	Cu$_B$ ligand
		Y, D[b], C[b]	Severe disruption of a_3-Cu$_B$	
*His334	VII	N, Y[b]	Severe disruption of a_3-Cu$_B$	Cu$_B$ ligand
*Thr352[c]	VIII	A, I[b]	a_3 environment disturbed, but iron-his stretch of a_3 evident	Close to a_3-Cu$_B$ center, possibly involved in H⁺ transfer or stabilization of oxygenated intermediates
Thr359	VIII	A	25% active; near wild-type optical and RR spectra, but minor alteration of the a_3-Cu$_B$ environment by FTIR	H⁺/H₂O pathway to the a_3-Cu$_B$ center
Lys362	VIII	M	a_3 iron-his stretch altered (*His*419 deprotonated?)	H⁺/H₂O pathway to the a_3-Cu$_B$ center
		R[b]	Enzyme unstable or poorly expressed	
His411	IX–X loop	A	80% active; metal centers normal; no Mn binding	Non-redox active metal ligand near active site
		N	a_3 environment severely disturbed; no Mn binding	
Asp412	IX–X loop	N, E[b]	30% active; a_3 iron-his stretch altered; no Mn binding	Non-redox active metal ligand near active site
Thr413	IX–X loop	N	80% active; metal centers normal	
Tyr414	IX–X loop	F	50% active; a_3-Cu$_B$ environment normal; heme *a* optically red-shifted	Possible member of H-bond network to heme *a* propionates
*His419	X	N, Y[b]	a_3-Cu$_B$ environment disrupted; a_3 iron-his stretch lost	a_3 ligand
*Phe420	X	V[b]	Partially active; minor alteration of a_3-Cu$_B$ environment	Unknown
*His421	X	N, Y[b], I[b]	Unstable protein; loss of α-band absorbance	Heme *a* ligand

[a] All mutants are inactive in electron transfer except where noted.
[b] Assayed in the membrane-bound form only; all other mutant oxidases have been purified.
[c] Completely conserved as Thr or Ser.
[d] An asterisk before the residue denotes a completely conserved residue among 33 oxidases.
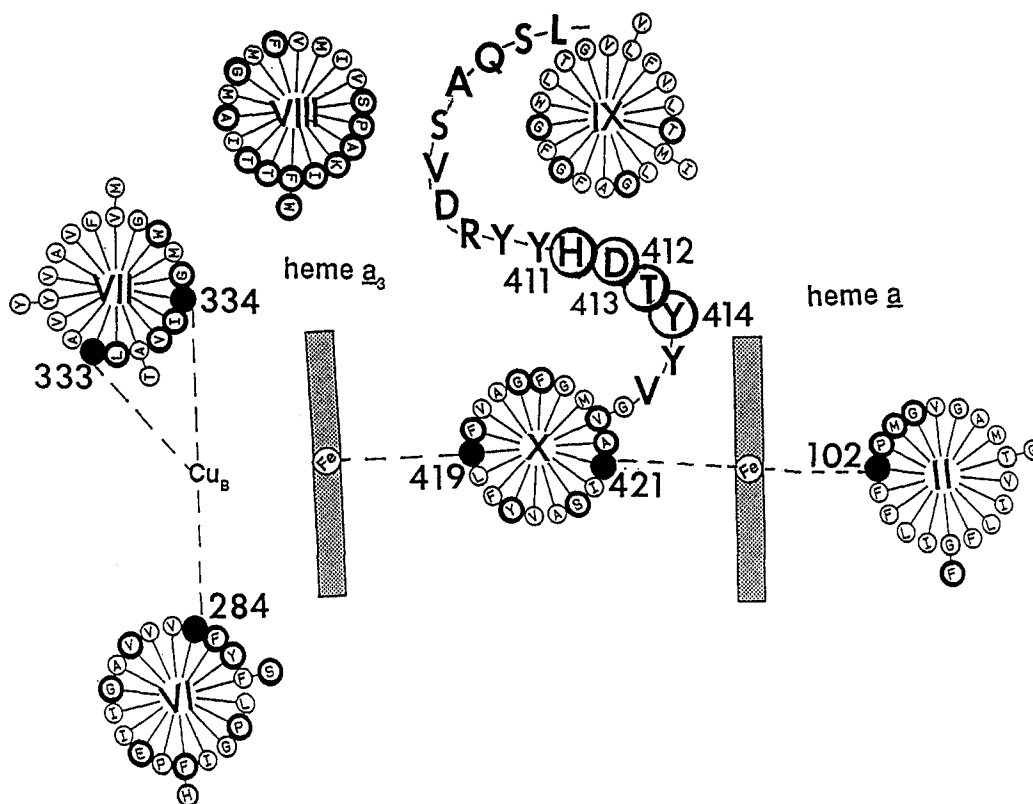
Fig. 3. A helical wheel model showing the ligation of heme a, heme a_3, and Cu_B by the six conserved histidines in subunit I of the *Rb. sphaeroides* oxidase. Conserved residues are in bold circles. Also included is the predicted extra-membrane sequence connecting helix IX and helix X.

stages of purification (Hosler, Tecklenburg, Shapleigh, Gennis, Babcock, and Ferguson-Miller, unpublished results). The *His284Ala* mutant shows some evidence of a native iron-histidine stretch in membrane-bound and partially purified states, whereas the *His419Asn* mutant does not. Apparently *His284Ala* can still adopt a native-like conformation in the appropriate lipid environment, even though other spectral signals show that the mutation disorders the binuclear center pocket. Since alanine cannot function as a metal ligand, the presence of an apparently native heme a_3 iron–histidine bond in *His284Ala* strongly favors the alternative model of *His*419 as the heme a_3 ligand. FTIR analysis on similar mutants of cytochrome *bo* (see Section 2.8) also supports the tentative assignment of *His*419 as the heme a_3 ligand.

A model that is consistent with these assignments depicts an arrangement of several of the transmembrane helices of COXI (Fig. 3 and see cover). It must be emphasized that this is a working model or pictorial aid. Furthermore, the assignment of ligands is predicated on the assumption that all of the ligands

are histidines. Although this assumption is strongly supported by spectroscopic evidence in the case of hemes a and a_3, the number and nature of the ligands of Cu_B are less certain (Powers *et al.*, 1981; Cline *et al.*, 1983; Scott *et al.*, 1986; Surerus *et al.*, 1992). Interpretation of the data must also take into account the possibility that the residue that is introduced functions as a metal ligand, or that the metal adopts an existing residue to serve as an alternative ligand in the mutant oxidase.

1.4. The Roles of Other Conserved Residues in COXI

Figure 1 shows a hypothetical arrangement of COXI in the membrane predicted from hydropathy plot analysis and supported by gene fusion experiments on the *bo*-type oxidase (see Section 2.6). Totally and highly conserved residues are also shown in this representation. Besides residues in the immediate vicinity of the designated metal ligands, there are several other regions of the polypeptide that suggest functional importance because of high levels of conservation. These include a hydrophilic face of

helix VIII, the extra-membranous loop between helix II and helix III, predicted to be cytoplasmic, and the loop between helix IX and helix X, predicted to be periplasmic. Mutational analysis of these and other regions is currently under way. Table II summarizes some of the findings obtained so far.

Mutants of several consecutive residues (*His*411, *Asp*412, *Thr*413, and *Tyr*414) in the IX–X loop affect the spectroscopic characteristics of heme *a* and heme *a₃*, supporting the model showing proximity of these centers (Hosler *et al.*, 1992a). Two residues in this loop, *His*411 and *Asp*412, are also apparently involved in binding manganese (see Section 1.1). A further role for this region in proton pumping has been investigated, with particular interest in *Asp*412, since a carboxylate residue, capable of rapid deprotonation, may be a necessary component of the proton pathway to the external phase. However, mutants in residues 411, 412, 413, and 414 show both electron transfer and proton pumping activity (Fetter, Hosler, Thomas, Gennis, and Ferguson-Miller, unpublished results). A proposed role for *Tyr*414 as a hydrogen bond donor to the formyl group of heme *a* (Saraste, 1990) is disproved by the finding that *Tyr*414*Phe* does not alter the intensity or position of the resonance Raman frequency attributed to that formyl stretch (Hosler, Shapleigh, Tecklenburg, Ferguson-Miller, and Gennis, unpublished results). The proximity of *Tyr*414 to heme *a* is, however, suggested by the absorption spectrum of heme *a* which is altered in the *Tyr*414*Phe* mutant.

The hydrophilic face of helix VIII is one of the most highly conserved regions of subunit I (Fig. 1) and may form part of the lining of a channel that conducts water and protons within the protein. Our current results favor a close interaction of this region with a heme *a₃*–Cu_B center that is located toward the outer side of the membrane (Fig. 3). Mutation of *Thr*352, with a predicted location close to the periplasmic or outer side of the membrane, to alanine, disrupts the heme *a₃* environment and eliminates catalytic activity. Substitution of alanine for *Thr*359, located near the center of the membrane, creates a partially active oxidase with heme *a₃* and the other metal centers apparently native. Interestingly, substitution of *Lys*362, located near the inner surface, with methionine has a specific effect (Table II) on the axial ligation of heme *a₃*, associated with loss of catalytic activity and altered CO binding. This supports the idea that this residue may play some role in proton or water access to the metal centers.

The proposed region providing the amino acid ligands of the heme *a₃*–Cu_B binuclear center (helices VI, VII, and X) has been subject to further mutational analysis, including *Tyr*288*Phe* and *Glu*286*Gln*. Both of these mutants have little or no activity. The *Tyr*288*Phe* mutant shows significant disruption of the binuclear center and shares many characteristics with *His*284*Ala*. Since *Tyr*288 is four residues (or one helical turn) below *His*284, it is well positioned to serve as a Cu_B ligand, perhaps transiently, as the geometry of Cu_B ligation changes during the redox cycle. The presence of a totally conserved proline between *His*284 and *Glu*286 suggests a disruption or distortion of the helix at this position that could result in a different relationship of *Glu*286 and *Tyr*288 with respect to the binuclear center than that shown in the helical model of Fig. 3. Whether sufficient distortion could occur to allow interaction between *Glu*286 and either Cu_B or heme *a₃* (Brown *et al.*, 1992) is an interesting question (see Conclusions). *Glu*286 is the only conserved carboxylate residue predicted to be in a membrane-spanning region of subunit I. Such acidic residues have been shown to be important in facilitating proton transport in other membrane proteins (Otto *et al.*, 1989; Henderson *et al.*, 1990; Takahashi and Wraight, 1991).

Cytochrome *bo* (Ubiquinol Oxidase) of *Escherichia coli*

2.1. Cytochrome bo Is a Five-Subunit Oxidase

Most, if not all, members of the heme-copper oxidase superfamily appear to have in common three core subunits that correspond to the three mitochondrially encoded subunits of the eukaryotic oxidases. In *E. coli*, these three subunits are encoded by the first three genes of the *cyo* operon. The entire operon contains five genes, corresponding to the five subunits of the purified oxidase: *cyo*A (subunit II), *cyo*B (subunit I), *cyo*C (subunit III), *cyo*D (subunit IV), and *cyo*E (subunit V) (Chepuri *et al.*, 1990b). Subunits IV and V are not related to nuclear-encoded subunits of the eukaryotic enzymes, but they are homologous to subunits or open reading frames associated with some prokaryotic *aa₃*-type cytochrome *c* oxidases (see Section 1.2) (Chepuri *et al.*, 1990b; Saraste *et al.*, 1991).

Previous studies have shown *E. coli* cytochrome *bo* to be a four-subunit enzyme (Matsishita *et al.*, 1984; Georgiou *et al.*, 1988; Puustiunen *et al.*, 1991;
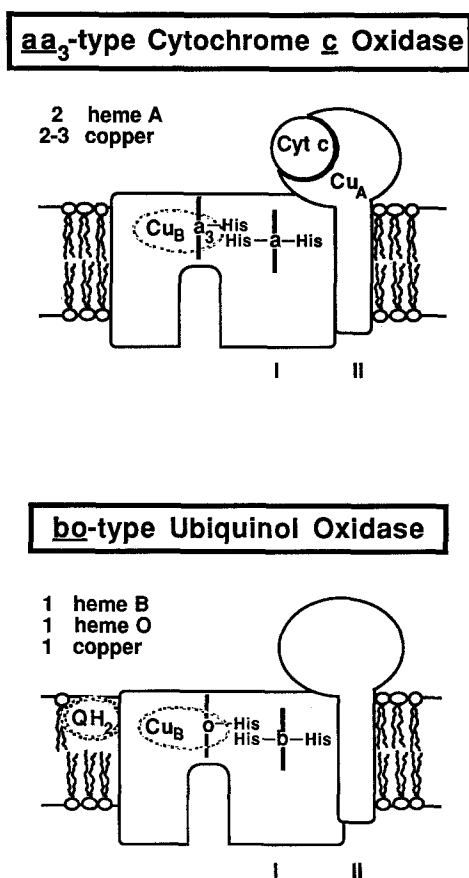
aa₃-type Cytochrome c Oxidase

2 heme A
2-3 copper

bo-type Ubiquinol Oxidase

1 heme B
1 heme O
1 copper

Fig. 4. Schematic showing subunits I and II of the aa₃-type cytochrome c oxidase and the bo-type ubiquinol oxidase.

Wu *et al.*, 1992). Alteration of the preparation procedure demonstrates a fifth subunit that has the molecular weight expected for the *cyoE* gene product (Mogi and Anraku, 1990; Minghetti *et al.*, 1992). The catalytic and spectroscopic properties of the four- and five-subunit forms of the enzyme appear to be virtually identical. Although subunit V is not an essential component for oxidase turnover, the *cyoE* gene product is essential for the assembly of the functional oxidase (see Section 2.6 and Mingnetti *et al.*, 1992).

Work on the aa₃-type cytochrome c from *P. denitrificans* has demonstrated that subunits I and II alone are sufficient for both electron transfer activity and proton pumping (Haltia *et al.*, 1991; Hendler *et al.*, 1991). The corresponding subunits of cytochrome *bo* are shown schematically in Fig. 4. Subunit I, which binds all three of the metals associated with the ubiquinol oxidases and three of the four metals associated with the cytochrome c oxidases, has been the focus of most of the mutagenesis studies to date

(Lemieux *et al.*, 1992; Minagawa *et al.*, 1992). The results are fully consistent with the conclusions based on the studies with the *Rb. sphaeroides* cytochrome c oxidase, presented in Section 1.

2.2. Cytochrome bo Is a Proton Pump

The *bo*-type oxidase catalyzes both scalar and vectorial proton translocation (Matsushita *et al.*, 1984; Puustinen *et al.*, 1989, 1991). The two-electron oxidation of quinol is associated with the release of two protons on the periplasmic side of the membrane. Concomitantly, the four-electron reduction of molecular oxygen of water is associated with the uptake of four protons, which presumably come from the cytoplasmic side of the membrane. Hence, chemical processes alone predict that during enzyme turnover one proton per electron will disappear from the cytoplasm and appear in the periplasm. This "scalar" mechanism is sufficient to account for the ratio of one H^+/e^-. However, studies of the *bo*-type oxidase in spheroplasts yield a ratio of $2\,H^+/e^-$ (Puustinen *et al.*, 1989, 1991). This is most reasonably explained by an additional vectorial mechanism similar to that observed in the aa₃-type cytochrome c oxidases (Wikström, 1989; Larsen *et al.*, 1992), involving the coupling of the redox process to movement of a second proton across the membrane.

It is noted that there is no report of the reconstituted purified *bo*-type oxidase functioning as a proton pump. Efforts to do so have yielded only the ratio of $1\,H^+/e^-$ expected for the simple scalar mechanism (Matsushita *et al.*, 1984). This may be the result of a scrambled orientation of the purified quinol oxidase in reconstituted phospholipid vesicles (Puustinen *et al.*, 1991) or loss of activity during purification. It is possible, though not probable, that the failure of this reconstituted, four-subunit preparation to function as a vectorial proton pump is due to the loss of subunit V.

2.3. Cytochrome bo Has Only One Copper

Metal analysis indicates that the purified oxidase contains two equivalents of iron and one equivalent of copper per mole of enzyme (Puustinen *et al.*, 1991; Minghetti *et al.*, 1992). The two irons are accounted for by the two heme components and the copper is associated with the binuclear center. The *bo*-type quinol oxidase does not contain Cu_A, the EPR-detectable component of the cytochrome c oxidases which is putatively ligated to residues within the hydrophilic

domain of subunit II (Fig. 4) (Blair *et al.*, 1983; Minghetti *et al.*, 1992). This is consistent with the fact that the amino acid residues that are probable ligands of Cu_A in the cytochrome *c* oxidases are not conserved in the sequence of subunit II of the quinol oxidase (Chepuri *et al.*, 1990b; Saraste, 1990; van der Oost *et al.*, 1992). One of the putative functions of Cu_A is to oxidize cytochrome *c*; since the *bo*-type oxidase exhibits no cytochrome *c* oxidase activity, the lack of Cu_A is not surprising. The fact, however, that the quinol oxidase functions as a vectorial proton pump makes it unlikely that Cu_A plays a critical role in the proton pumping mechanism, as has been proposed for the cytochrome *c* oxidases (Gelles *et al.*, 1987).

2.4. Cytochrome bo Has a Heme-Copper Binuclear Center

Electron spin resonance studies of the heme components of the *bo*-type oxidase show the presence of a heme-copper binuclear center, a diagnostic feature of this entire superfamily of oxidases (Salerno *et al.*, 1989, 1990). A redox titration shows an EPR signal typical of a high-spin heme, but at high potential ($+400$ mV) this signal is quenched. This is explained by the presence of a nearby copper (Cu_B) which, upon oxidation, is electronically coupled to the heme iron in such a way that the EPR signal is eliminated. This behaviour is also observed with cytochrome *c* oxidise (van Gelder and Beinert, 1969).

A second technique that demonstrates the presence of a heme-copper binuclear center is Fourier transform infrared (FTIR) spectroscopy, in which CO bound to the oxidase is used as a probe (Fiamingo *et al.*, 1982, 1986). The stretching frequency of the CO bond is sensitive to the environment of the CO, including its ligation state. When bound to the heme *o* component of the *bo*-type oxidase, the CO stretching frequency is $1959\,\mathrm{cm}^{-1}$ (Chepuri *et al.*, 1990a; Hill *et al.*, 1992). After photolysis, the bound CO shifts from heme *o* to Cu_B, and the FTIR band is centered at $2063\,\mathrm{cm}^{-1}$. The difference spectrum for cytochrome *bo* is shown in Fig. 2 and compared with that from the *Rb. sphaeroides* oxidase. These data demonstrate definitively the presence of a heme-copper binuclear center in cytochrome *bo*.

2.5. Cytochrome bo Contains Two Heme Components

Extraction of heme from the purified *bo*-type

oxidase reveals two equivalents of heme, corresponding to the two iron equivalents. Earlier work identified the two hemes as being protoheme IX (heme B), based on simple spectroscopic critieria (Kita *et al.*, 1984; Matsushita *et al.*, 1984). Closer examination, however, indicated that one of the two heme components is chemically distinct from heme B, and this new heme has been named heme O (Puustinen and Wikström, 1991; Wu *et al.*, 1992). The structures of heme B, heme O, and heme A are shown in Fig. 5.. Heme O is a modification of heme B, with a hydroxylfarnesyl side-chain addition (Wu *et al.*, 1992). This same modification is found in heme A, which differs from heme O by the addition of a formyl group. The formyl substituent is responsible for shifting the peak of the alpha band from about 560 nm in cytochrome *bo* to 603–606 nm in cytochrome *aa₃*.

The heme B prosthetic group of cytochrome *bo* is normally present as the low-spin six-coordinate cytochrome b_{562} component. This component is responsible for virtually all of the visible absorption of the oxidase, and has a split alpha band with peaks at 555 and 563.5 nm (Puustinen *et al.*, 1991; Minghetti *et al.*, 1992). In some strains of *E. coli* that overproduce the *bo*-type oxidase due to the presence of the *cyo* operon on a multicopy plasmid, heme O can substitute for heme B at this locus in the enzyme (Puustinen *et al.*, 1992). Depending on growth conditions, the enzyme can contain up to two equivalents of heme O, although the substitution of heme O for heme B has very little effect on the catalytic function of the oxidase. Hence, this is a promiscuous heme binding locus, although under normal physiological conditions in a wild-type strain heme B is always found at this site (Puustinen *et al.*, 1992).

The proper assembly of the oxidase requires the *cyo*E gene product (homologous to COX10 of yeast; see Section 1.2), as demonstrated by truncating the *cyo* operon so that *cyo*E is not expressed. The result is the assembly of a non-functional oxidase in the *E. coli* membrane. FTIR spectroscopy shows that the binuclear center is abnormal, and HPLC analysis indicates that heme O is absent from the membranes (Hill *et al.*, 1992). Whereas heme O can substitute for heme B to yield an active enzyme, the reverse substitution yields an inactive enzyme, indicating that cytochrome *bo* does not tolerate heme B in the binuclear center. Although the presence of subunit V (*cyo*E gene product) is not essential for activity of the purified enzyme, it is essential for correct assembly. This gene product may be required for the insertion of
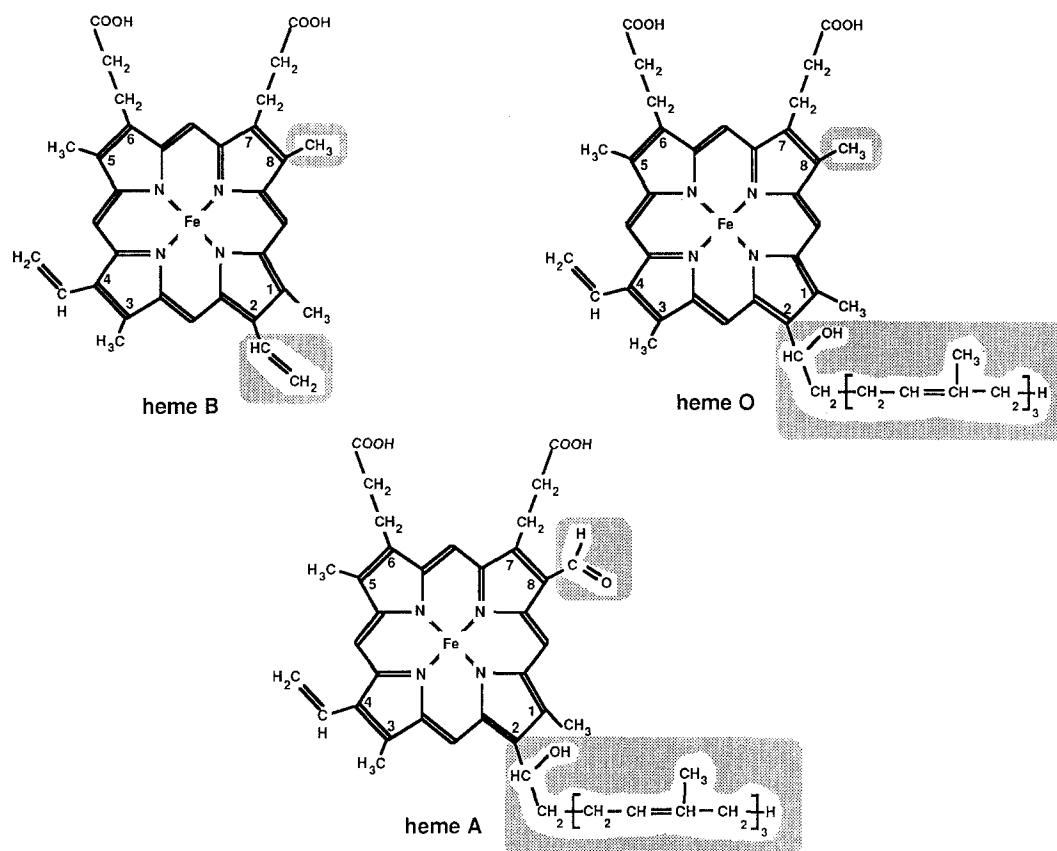
Fig. 5. The structures of heme *B*, heme *O*, and heme *A*.

heme O into the binuclear center, or for the biosynthesis of heme O from heme B.

2.6. Subunit topology and Two-Dimensional Modelling

The hydropathy profiles of the five subunits of the *bo*-type oxidase indicate that each contains multiple transmembrane spans (Chepuri *et al.*, 1990b). Based on the known structures of bacteriorhodopsin (Henderson *et al.*, 1990) and the bacterial photosynthetic reaction centers (Deisenhofer and Michel, 1989; Feher *et al.*, 1989), it is reasonable to assume that the transmembrane spans are helices with a minimum length of about 20 residues. The number and approximate boundaries of each putative transmembrane alpha helix was determined experimentally using the gene fusion approach (Chepuri and Gennis, 1990). This technique can identify regions of each polypeptide that are on or near the periplasmic side of the membrane, and those portions of each polypeptide that are on the cytoplasmic surface. The results are internally

consistent and are also consistent with the relatively limited data available from other approaches.

Subunit I: The data indicate that subunit I of the *E. coli* oxidase has 15 transmembrane spans. Twelve of these putative helical spans correspond to those shown in Fig. 1. The *E. coli* subunit, however, has extentions on both the N- and C-termini compared to the homologous subunit from *Rb. sphaeroides* or beef. On the N-terminus, there is one additional transmembrane span, which places the amino terminal residue on the periplasmic side; on the C-terminus, there are two additional transmembrane spans. Similar extensions are found in several of the bacterial cytochrome *C* oxidases (Ishizuka *et al.*, 1990; Saraste *et al.*, 1991). It is interesting to note that in those cases where subunit I has the two additional transmembrane spans on the C-terminus, subunit III has two fewer on the N-terminus. Since the gene encoding subunit III in *E. coli* immediately follows that encoding subunit I, it is easy to rationalize how a transfer might have occurred at the genetic level (see also Fee *et al.*, this volume). However, there is little amino acid sequence homology

to confidently conclude that the last two spans of *E. coli* subunit I correspond to the first two spans normally found in subunit III.

There are no data apart from those from the gene fusion experiments that define which portions of subunit I are on the inner or outer side of the membrane or which define the number of membrane-spanning domains.

Subunit II: The gene fusions with the *E. coli* subunit II show that this subunit has both the N- and C-termini on the periplasmic side of the membrane, with two membrane-spanning helices in between (Chepuri and Gennis, 1990). There is a large hydrophilic domain on the C-terminus which is the likely site for the Cu$_A$ ligation and cytochrome *c* interaction in *aa₃*-type oxidases. The topology suggested by the gene fusions with the *E. coli* subunit is identical to that determined by more classical biochemical techniques for the equivalent subunit from beef and *P. denitrificans* (Bisson *et al.*, 1982; Finel, 1988; Saraste, 1990).

Subunit III: The *E. coli* subunit is predicted to have five transmembrane spans with the N-terminus on the cytoplasmic side of the membrane. As indicated above, in most other organisms including *Rb. sphaeroides* (Cao *et al.*, 1992), subunit III is larger and contains two additional predicted spans on the N-terminal side.

Subunits IV and V: Subunits IV and V have three and seven transmembrane spans, respectively. In each case the N-terminus is predicted to be on the inner side of the membrane (Chepuri and Gennis, 1990).

The results of the gene fusion experiments indicate that the C-terminus of subunit II and the N-terminus of *E. coli* subunit I are both on the periplasmic side of the membrane. Similarly, the C-terminus of subunit I and the N-terminus of subunit III are expected to be on the cytoplasmic side of the *E. coli* membrane. The gene order, *cyo*A–*cyo*B–*cyo*C (subunit II–I–III), facilitates the construction of in-frame fusions to link subunits I, II, and III to form a single polypeptide. In principle, this is possible because the topology places the N- and C-termini to be fused on the same side of the membrane for each pair of polypeptides. This experiment was performed successfully: the resulting product is an active oxidase with subunits I, II, and III fused together (Ma and Gennis, unpublished results). Minimally, this experiment confirms the two-dimensional folding pattern already described.

The two-dimensional models of the subunits form the backdrop that is essential for the structural

interpretation of the results from site-directed mutagenesis. The latter, as indicated below, provides information concerning the three-dimensional relationship of portions of the oxidase.

2.7. Mutagenesis of Subunit II

The bulk of the mutagenesis experiments to date have involved residues in subunit I. However, an important set of experiments has been initiated investigating the structure and function of subunit II. A set of residues which are thought to be the ligands to Cu$_A$ in the cytochrome *c* oxidases (Stevens *et al.*, 1982; Blair *et al.*, 1983; Li *et al.*, 1987) was placed in the hydrophilic domain of subunit II of the *E. coli* oxidase. EPR spectra of the resulting subunit demonstrate the restoration of a Cu$_A$-like center (van der Oost *et al.*, 1992). These data strongly suggest that the three-dimensional folding pattern of the *E. coli* subunit is similar to that of cytochrome *c* oxidase, although the function of this subunit is not conserved.

2.8. Site-Directed Mutagenesis and Three-Dimensional Modelling of Subunit I

Many mutations have been made in subunit I of the *E. coli* oxidase. The results are completely compatible with the data obtained with the mutations in the equivalent residues of *Rb. sphaeroides* cytochrome *c* oxidase (Section 1). The results obtained with the *E. coli* oxidase independently support the model shown in Fig. 3. Helices II, VI, VII, and X are clearly involved directly in ligating the metals within subunit I (Lemieux *et al.*, 1992; Minagawa *et al.*, 1992), and residues on the polar face of Helix VIII are important for catalytic function (Thomas and Gennis, unpublished results). Some of these data are summarized in Table III.

Metal Binding. All substitutions for any of the six totally conserved histidine residues in subunit I are catalytically inactive (Lemieux *et al.*, 1992; Minagawa *et al.*, 1992). In most cases, the mutant enzyme is assembled and overproduced in the *E. coli* membrane. Spectroscopic techniques, including optical absorption, EPR, and FTIR spectroscopies, have been particularly valuable in deciphering the nature of each lesion. *His*106 (Helix II) and *His*421 (Helix X) are the ligands of the low-spin heme *b*$_{562}$ component of the oxidase, as indicated by loss of this heme when either of these histidines is replaced (Lemieux *et al.*, 1992; Minagawa *et al.*, 1992). The equivalent histidines have

Table III. Some mutants in Subunit I of Cytochrome *bo* Oxidase from *E. coli*

Subunit I residue[d]	Helix	Mutation(s)	Phenotype of mutants[a]	Proposed role of residue
*His106	II	G, L	Loss of α-band absorbance; no low-spin EPR	Heme *b* ligand
*Met110	II	I	Complements; wild-type FTIR spectrum	Nonessential
Asn277	VI	D, Y	Complement; have wild-type spectra	Nonessential
*His284	VI	G, L C, N, Q, W, Y	FTIR Fe–CO similar to wild-type; low CO binding Low CO binding	Possible Cu_B ligand
Glu286	VI	A Q	Not active Partially active with near wild-type FTIR	Possible resting state bridging ligand
*Tyr288	VI	A, F, S	Loss of Cu_B by FTIR	Possible Cu_B ligand
*His333	VII	C, L, M, N, Q, R	Loss of Cu_B by FTIR and EPR	Cu_B ligand
*His334	VII	C, L, M, N, Q, R	Loss of Cu_B by FTIR and EPR	Cu_B ligand
*Thr352[b]	VIII	A S	Disrupts binuclear center Complements	Role in H^+ transfer and/or stabilization of oxygenated intermediates
Pro358	VIII	A	Complements	Nonessential
Thr359	VIII	A S	Oxidase inactive, but all metal centers present Complements	H^+/H_2O pathway
Lys362	VIII	A, M, Q	All metal centers present but inactive	H^+/H_2O pathway
His411	IX–X loop	G L	Complements Does not complement	Nonessential
*His419	X	N C, D, G, L, M, Q, Y	Binuclear center with shifted Fe–CO and Cu–CO frequencies Binuclear center disrupted	Heme *o* ligand
*His421	X	G, L	Loss of α-band absorbance; no low spin EPR	Heme *b* ligand

[a]Unless noted by the term "complements," all mutations are inactive by the specific criterion of being unable to support aerobic growth in the *cyo cyd* host strain RG129 (Au and Gennis, 1987). This strain cannot grow aerobically without an active terminal oxidase that is plasmid-encoded (see Lemieux *et al.*, 1992). Inactivity by this criterion does not necessarily mean a complete loss of biochemical function.
[b]Conserved as Thr or Ser.
[c]Residue numbers are identical to *Rb. sphaeroides* except for *His*106 and *Met*110, which are *His*102 and *Met*106 in *Rb. sphaeroides*.
[d]Asterisks denote completely conserved residues.

been shown to be the ligands for the analogous low-spin heme (heme *a*) in *Rb. sphaeroides* cytochrome *c* oxidase (Section 1.3; Shapleigh *et al.*, 1992b). Substitutions for either of the two adjacent histidines in

Helix VII (*His*333 and *His*334) results in the elimination of Cu_B, as indicated by FTIR, EPR, and atomic absorption measurements (Calhoun, Lemieux, Alben, and Gennis, unpublished data; Minagawa *et al.*,

1992). The assignment of either *His*284 or *His*419 as the ligand to the high-spin heme *o* has, until recently, been more problematic (Lemieux *et al.*, 1992; Minagawa *et al.*, 1992). However, it has been observed by FTIR spectroscopy that *His*284 can be replaced by a glycine or leucine without perturbing the band width and only slightly perturbing the center frequency of CO bound to the heme, whereas the signal expected for CO bound to Cu_B is not observed (Calhoun, Thomas, Lemieux, Alben, and Gennis, unpublished results). This is easier to rationalize if *His*284 is assigned as a Cu_B ligand and is not the axial ligand to the CO-binding heme. Hence, the model shown in Fig. 3 is strongly favored, in which *His*419 is shown as the high-spin heme (*o* or a_3) ligand, and *His*284 is a third potential Cu_B ligand. Indirect support for this model comes from the observation that substitution of *Tyr*288, located four residues (or one helical turn) below *His*284 in Helix VI, by phenylalanine also results in the loss of the Cu_B FTIR signal (Thomas and Gennis, unpublished results). Thus, *Tyr*288 must be considered as a possible ligand to Cu_B. Similar results have been obtained with the *Rb. sphaeroides* oxidase (Section 1.3). Possible sulfur ligation to Cu_B has been previously suggested (Powers *et al.*, 1981). However, the only sulfur-containing residue that is totally conserved in subunit I is *Met*110 (*E. coli* notation) in Helix II. Due to the assignment of *His*106 of Helix II as a ligand for heme b_{562} (heme *a*), *Met*110 is unlikely to ligand Cu_B. In fact, mutagenesis data show that *Met*110 is not an essential residue in the *E. coli* oxidase (Calhoun, Lemieux, Thomas, and Gennis, unpublished results).

The Polar Face of Helix VIII. Substitution of *Thr*352 in Helix VIII by alanine results in complete loss of catalytic activity (Thomas and Gennis, unpublished results). This is also associated with severe perturbation of the binuclear center, suggesting that *Thr*352 may be located at or very close to the heme *o*-Cu_B binuclear center. This is easily accommodated by the model in Fig. 3 and is consistent with the results obtained with mutations in the equivalent position in the cytochrome *c* oxidase of *Rb. sphaeroides* (Section 1.4). Substitution of *Thr*359 by alanine or of *Lys*362 by methionine causes a severe loss of catalytic activity, but in neither of these cases is there any perturbation of the FTIR spectra to indicate that the metal centers are directly affected by the mutation (Thomas, Alben, and Gennis, unpublished results). The equivalent *Lys*362Met mutation in *Rb. sphaeroides*, however, does perturb the heme a_3 resonance Raman spectrum
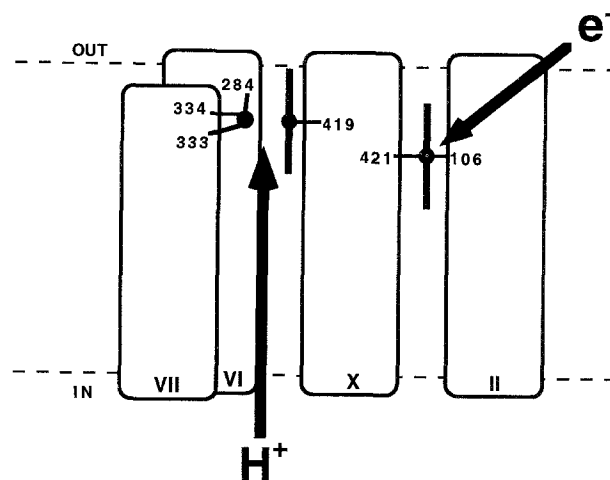

Fig. 6. An illustration of the proposed organization of the three metals in subunit I in relationship to transmembrane helices, II, VI, VII, and X, which contain the metal ligands. Helix VIII, proposed to form part of a hydrophilic channel leading to the heme a_3-Cu_B center, is not shown.

(Table II). Tentatively, the most reasonable explanation of these results is that residues in this portion of the protein are important for delivering protons to the site where oxygen is reduced to water and/or for providing a path for water to exit the enzyme. This channel may convey both substrate protons and those that are ultimately transported across the membrane.

CONCLUSIONS

The mutagenesis results have confirmed the close relationship between the cytochrome *c* oxidases and the *E. coli* ubiquinol oxidase. The picture of subunit I that is emerging places both hemes and Cu_B at approximately the same level in the membrane and near the periplasmic side, which corresponds to the intermembrane space in the mitochondrion. This aspect is emphasized in the drawing in Fig. 6. The most likely ligand of the high-spin heme is *His*419 of Helix X. Cu_B is postulated to be ligated by residues in Helix VII (*His*333 and *His*334) and possibly by residues in Helix VI (*His*284 and *Tyr*288). The heme a_3-Cu_B pocket also includes residues from Helix VIII (*Thr*352).

Conceivably, the combination of amino acid residues that ligate the heme a_3-Cu_B center may reorganize or change during turnover of the oxidase (see also Woodruff and Rousseau *et al.*, this volume). One or more of the residues in Helix VI and VII that have been invoked as Cu_B ligands and are also positioned near the distal side of heme a_3 (or heme *o*)

may interact directly with the heme iron under certain conditions. For example, $His284$ and $Tyr288$ could participate in a ligand switching mechanism between the heme iron and Cu_B; both could be involved in proton pumping. $His284$ might also serve as the bridging ligand postulated to couple heme a_3 (or o) and Cu_B, particularly since the strength of the coupling between the two metals is suggestive of a histidine bridge (Palmer et al., 1976; Tweedle et al., 1978). Alternatively the so-called resting state of the oxidase might result from an interaction of $Glu286$ (Helix VI) with the metals of the binuclear center (Brown et al., 1992). $Glu286$ follows the sequence $Gly283-His284-Pro285$, which is highly conserved in the sequences of subunit I. A search for the sequence $Gly-His-Pro$ in soluble proteins of known structure shows that it is found in turns. Hence, this portion of the polypeptide may not be simply helical, as we show in the models (Figs. 1 and 6). The possibility of different conformational states, for example "fast" vs. "slow" enzyme (Baker et al., 1987; Moody et al., 1991), being manifestations of the interactions of $His284$ and $Glu286$ with the metals in the binuclear center is intriguing. Future studies may clarify some of these issues.

An interesting feature of the developing model is that heme a_3 (or o) and heme a (or b_{562}) are both postulated to be ligated by residues within Helix X at essentially the same level in the membrane, close to the periplasmic (outer) side. Hence, electron flow from heme a to the binuclear center can occur through sigma bonds (Wuttke et al., 1992) across Helix X, essentially parallel to the surface of the membrane. The protons needed to form water from oxygen must be transported from the opposite side of the membrane via some structure within the enzyme, and the resulting product, water, must similarly be transported away from the binuclear center. The highly conserved polar residues found in Helix VIII are strong candidates for forming part of such a hydrophilic channel.

Our proposal of $His419$ as the ligand of heme a_3, rather than $His284$ (Shapleigh et al., 1992b), leads to the current model (Fig. 3) in which Cu_B is no longer located between the two hemes. This would appear to conflict with the electron transfer pathway of heme a to Cu_B to heme a_3 (Babcock and Wikstrom, 1992). One can envision, however, ligand rearrangements associated with Cu_B reduction and oxidation (Larsen et al., 1992) that affect the redox potential of heme a_3 (or Cu_B) and thus control the pathway. For example, $Tyr288$ may ligand reduced but not oxidized Cu_B;

unliganded $Tyr288$ could interact with the porphyrin ring of heme a_3 to alter the redox potential of the heme (see the front cover of this volume). A similar mechanism could be envisioned for $His284$. Ligand switching at the heme a_3 iron associated with oxygen binding is also proposed as a mechanism for control of electron flow, in this case by directly changing the pathway (see articles by Woodruff and Rousseau et al., this volume).

The combination of mutagenesis techniques and biophysical methods is particularly powerful, especially with the rich array of techniques available for studying metalloproteins such as these oxidases. Even in the absence of the long sought, high-resolution X-ray structure, much can be learned and the future promises to be interesting.

ACKNOWLEDGMENT

REFERENCES

Alben, J. O., Moh, P. P., Fiamingo, F. G., and Altschuld, R. A. (1981). Proc. Natl. Acad. Sci. USA 78, 234–237.

Albracht, S. P. J., van Verseveld, H. W., Hagen, W. R., and Kalkman, M. L. (1980). Biochim. Biophys. Acta 593, 173–186.

Anraku, Y., and Gennis, R. B. (1987). Trend. Biochem. Sci. 12, 262–266.

Au, D. C.-T., and Gennis, R. B., (1987). J. Bacteriol. 169, 3237–3242.

Babcock, G. T., and Wikstrom, M. (1992). Nature (London), 356, 301–309.

Baker, G. M., Noguchi, M., and Palmer, G. (1987). J. Biol. Chem. 262, 595–604.

Berry, E. A., and Trumpower, B. L. (1985). J. Biol. Chem. 260, 2458–2467.

Bisson, R., Steffens, G. C. M., and Buse, G. (1982). J. Biol. Chem. 257, 6716–6720.

Blair, D. F., Martin, C. T., Gelles, J., Wang, H., Brudvig, G. W., Stevens, T. H., and Chan, S. I. (1983). Chem. Scri. 21, 43–53.

Brown, S., Moody, A. J., Jeal, A. E., Bourne, R. M., Mitchell, J. R., and Rich, P. R. (1992). EBEC 7, 39.

Cao, Shapleigh, J., Gennis, R., Revzin, A., and Ferguson-Miller, S. (1991). Gene 101, 133–137.

Cao, J., Hosler, J., Shapleigh, J., Revzin, A., and Ferguson-Miller, S. (1992). J. Biol. Chem. 267, 24273–24278.

Caughey, W. S., Bayne, R. A. and McCoy, S. (1970) J. Chem. Soc. 950–951.

Chepuri, V., and Gennis, R. B. (1990). J. Biol. Chem. 265, 12978–12986.

Chepuri, V., Lemieux, L., Hill, J., Alben, J. O., and Gennis, R. B. (1990a). *Biochim. Biophys. Acta* **1018**, 124–127.

Chepuri, V., Lemieux, L. J., Au, D. C.-T., and Gennis, R. B. (1990b). *J. Biol. Chem.* **265**, 11185–11192.

Cline, J., Reinhammar, B., Jensen, P., Venters, R., and Hoffman, B. M. (1983). *J. Biol. Chem.* **258**, 5124–5128.

Deisenhofer, J., and Michel, H. (1989). *Science* **245**, 1463–1473.

Einarsdóttir, O., Choc, M. G., Weldon, S., and Caughey, W. S. (1988). *J. Biol. Chem.* **263**, 13641–13654.

Erecinska, M., Wilson, D. F., and Blasie, J. K. (1979). *Biochim. Biophys. Acta* **545**, 352–364.

Feher, G., Allen, J. P., Okamura, M. Y., and Rees, D. C. (1989). *Nature (London)* **339**, 111–116.

Fiamingo, F. G., Altschuld, R. A., Moh, P. P., and Alben, J. O. (1982). *J. Biol. Chem.* **257**, 1639–1650.

Fiamingo, F. G., Altschuld, R. A., and Alben, J. O. (1986). *J. Biol. Chem.* **261**, 12976–12987.

Fiamingo, F. G., Jung, D. W., and Alben, J. O. (1990). *Biochemistry* **29**, 4627–4633.

Finel, M. (1988). *FEBS Lett.* **236**, 415–419.

Gelles, J., Blair, D. F., and Chan, S. I. (1987). *Biochim. Biophys. Acta* **853**, 205–236.

Gennis, R. B. (1991). *Biochim. Biophys. Acta* **1058**, 21–24.

Georgiou, C., Cokic, P., Carter, K., Webster, D. A., and Gennis, R. B. (1988). *Biochim. Biophys. Acta* **933**, 179–183.

Haltia, T. (1992). *Biochim. Biophys. Acta* **1098**, 343–350.

Haltia, T., Saraste, M., and Wikström, M. (1991). *EMBO J.* **10**, 2015–2021.

Henderson, R., Baldwin, J. M., Ceska, T. A., Zemlin, F., Beckmann, E., and Downing, K. H. (1990). *J. Mol. Biol.* **213**, 899–929.

Hendler, R. W., Pardhasaradhi, K., Reynafarje, B., and Ludwig, B. (1991). *Biophys. J.* **60**, 415–423.

Hill, J., Goswitz, V. C., Calhoun, M., Garcia-Horsman, J. A., Lemieux, L., Alben, J. O., and Gennis, R. B. (1992). *Biochemistry*, in press.

Hosler, J., Fetter, J., Shapleigh, J., Espe, M., Thomas, J., Kim, Y., Gennis, R., Babcock, G., and Ferguson-Miller, S. (1992a). *EBEC* **7**, 38.

Hosler, J. P., Fetter, J., Tecklenberg, M. M. J., Espe, M., Lerma, C., and Ferguson-Miller, S. (1992b). *J. Biol. Chem.* **267**, 24264–24272.

Ishizuka, M., Machida, K., Shimada, S., Mogi, A., Tsuchiya, T., Ohmori, T., Souma, Y., Gonda, M. A., and Sone, N. (1990). *J. Biochem.* **108**, 866–873.

Kahlow, M. A., Zuberi, T. M., Gennis, R. B., and Loehr, T. M. (1991). *Biochemistry* **30**, 11485–11489.

Kita, K., Konishi, K., and Anraku, Y. (1984). *J. Biol. Chem.* **259**, 3368–3374.

Larsen, R. W., Pan, L.-P., Musser, S. M., Li, Z., and Chan, S. I. (1992). *Proc. Natl. Acad. Sci. USA* **89**, 723–727.

Lemieux, L. J., Calhoun, M. W., Thomas, J. W. Ingledew, W. J., and Gennis, R. B. (1992). *J. Biol. Chem.* **267**, 2105–2113.

Li, P. M., Gelles, J., Chan, S. I., Sullivan, R. J., and Scott, R. A. (1987). *Biochemistry* **26**, 2091–2095.

Matsushita, K., Patel, L., and Kaback, H. R. (1984). *Biochemistry* **23**, 4703–4714.

Minagawa, J., Mogi, T., Gennis, R. B., and Anraku, Y. (1992). *J. Biol. Chem.* **267**, 2096–2104.

Minghetti, K. C., Goswitz, V. C., Gabriel, N. E., Hill, J. J., Barassi, C., Georgiou, C. D., Chan, S. I., and Gennis, R. B. (1992). *Biochemistry* **31**, 6917–6924.

Mogi, T. and Anraku, Y. (1990). In *International Symposium on Bioenergetics of Proton Pumps: Biochemistry, Cell Biology, and Molecular Pathology* (Fuku, T., Futai, M., Maeda, M., Moriyama, Y., and Tanizawa, K., eds.), Osaka University Press, Osaka, Japan, pp. 96–99.

Moody, A. J., Cooper, C. E., and Rich, P. E. (1991). *Biochim. Biophys. Acta* **1059**, 189–207.

Nicholls, P., and Sone, N. (1984). *Biochim. Biophys. Acta* **767**, 240–247.

Nobrega, M. P., Nobrega, F. G., and Tzagoloff, A. (1990). *J. Biol. Chem.* **265**, 14220–14226.

Otto, H., Marti, T., Holz, M., Mogi, T., Lindau, M., Khorana, H. G., and Heyn, M. P. (1989). *Proc. Natl. Acad. Sci. USA* **86**, 9228–9232.

Palmer, G., Babcock, G. T., and Vickery, L. E. (1976). *Proc. Natl. Acad. Sci. USA* **73**, 2206–2210.

Powers, L., Chance, B., Ching, Y., and Angiolillo, P. (1981). *Biophys. J.* **34**, 465–498.

Puustinen, A., and Wikström, M. (1991). *Proc. Natl. Acad. Sci. USA* **88**, 6122–6126.

Puustinen, A., Finel, M., Virkki, M., and Wikström, M. (1989). *FEBS Lett.* **249**, 163–167.

Puustinen, A., Finel, M., Haltia, T., Gennis, R. B., and Wikström, M. (1991). *Biochemistry* **30**, 3936–3942.

Puustinen, A., Morgan, J. E., Verkhovsky, M., Thomas, J. W., Gennis, R. B., and Wikström, M. (1992). *Biochemistry* **31**, 10363–10369.

Raitio, M., Jalli, T., and Saraste, M. (1987). *EMBO J.* **6**, 2825–2833.

Salerno, J. C., Bolgiano, B., and Ingledew, W. J. (1989). *FEBS Lett.* **247**, 101–105.

Salerno, J. C., Bolgiano, B., Poole, R. K., Gennis, R. B., and Ingledew, W. J. (1990). *J. Biol. Chem.* **265**, 4364–4368.

Saraste, M. (1990). *Q. Rev. Biophys.* **23**, 331–366.

Saraste, M., Metso, T., Nakari, T., Jalli, T., Lauraeus, M., and Van der Oost, J. (1991). *Eur. J. Biochem.* **195**, 517–525.

Scott, R. A., Schwartz, J. W., and Cramer, S. (1986). *Biochemistry* **25**, 5546–5555.

Seelig, A., Ludwig, B., Seelig, J., and Schatz, G. (1981). *Biochim. Biophys. Acta* **636**, 162–167.

Shapleigh, J. P., and Gennis, R. B. (1992). *Mol. Microbiol.* **6**, 635–642.

Shapleigh, J. P., Hill, J. J., Alben, J. O., and Gennis, R. B. (1992a). *J. Bacteriol.* **174**, 2338–2343.

Shapleigh, J. P., Hosler, J. P., Tecklenburg, M. M. J., Kim, Y., Babcock, G. T., Gennis, R. B., and Ferguson-Miller, S. (1992b). *Proc. Natl. Acad. Sci. USA* **89**, 4786–4790.

Steinrücke, P., Gerhus, E., Jetzek, M., Turba, A., and Ludwig, B. (1991a). *J. Bioenerg. Biomembr.* **23**, 227–239.

Steinrücke, P., Gerhus, E., and Ludwig, B. (1991b). *J. Biol. Chem.* **266**, 7676–7681.

Stevens, T. H., Martin, C. T., Wang, H., Brudvig, G. W., Scholes, C. P., and Chan, S. I. (1982). *J. Biol. Chem.* **257**, 12106–12113.

Surerus, K. K., Oertling, W. A., Fan, C., Gurbiel, R. J., Einarsóttir, O., Antholine, W. E., Dyer, R. B., Hoffman, B. M., Woodruff, W. H., and Fee, J. A. (1992). *Proc. Natl. Acad. Sci. USA* **89**, 3195–3199.

Takahashi, E., and Wraight, C. A. (1991). *Biochemistry* **31**, 855–866.

Tweedle, M F., Wilson, L. J., Garcia-Iniguez, L., Babcock, G.T., and Palmer, G. (1978). *J. Biol. Chem.* **253**, 8065–8071.

Tzagoloff, A., Capitganio, N., Nobrega, M. P., and Gatti, D. (1990). *EMBO J.* **9**, 2759–2764.

van der Oost, J., Pappalainen, P., Musacchio, A., Warne, A., Lemieux, L., Rumbley, J., Gennis, R. B., Aasa. R., Pascher, T., Malmström, B. G., and Saraste, M. (1992). *EMBO J.* **11**, 3209–3217.

van Gelder, B. F., and Beinert, H. (1969). *Biochim. Biophys. Acta* **189**, 1–24.

Wikström, M., Saraste, M. and Penttitä, T. (1985) in *The Enzymes of Biological Membranes* (Martonosi, A., ed.) Vol. 4, Plenum Press, NY, pp. 111–148.

Wikström, M. (1989). *Nature (London)* **338**, 776–778.

Wu, W., Chang, C. K., Varotsis, C., Babcock, G. T., Puustinen, A.,
      and Wikström, M. (1992). *J. Am. Chem. Soc.* **114,** 1182–1187.
Wuttke, D. S., Bjerrum, M. J., Winkler, J. R., and Gray, H. (1992).

Science **256,** 1007–1009.
Yoshida, T., and Fee, J. A. (1984). *J. Biol. Chem.* **259,** 1031–1036.